Anal. Chem. **2000,** *72,* 2087−2092

Analysis of Solids by Laser Ablation and Resonance-Enhanced Laser-Induced Plasma Spectroscopy

S. Y. Chan and N. H. Cheung*

Department of Physics, Hong Kong Baptist University, Waterloo Road, Kowloon, Hong Kong, People's Republic of China

An analytical technique based on resonance-enhanced laser-induced plasma spectroscopy was demonstrated. Pellets of potassium iodate containing trace amounts of sodium were ablated by a 532-nm laser pulse in air. After 30 ns, the plasma plume was intercepted by a 404.4-nm laser pulse to resonantly photoionize the potassium atoms in the vapor plume. The 589-nm emissions of the sodium were found to be significantly enhanced. The enhancement was shown to depend critically on the profile of the 532-nm beam as well as the spatial overlap of the two laser pulses. Using this double-pulse scheme, the mass detection limit for sodium was estimated to be about 200 pg, which was five times better than that obtained by using the 532-nm laser pulse alone.

Laser-induced breakdown spectroscopy (LIBS) involves the ablation of a material target by an intense laser pulse. The microplasma produced will emit spectral fingerprints of the elements in the sample.[1] An extremely versatile and convenient analytical probe can therefore be devised. But its performance is plagued by poor reproducibility and low sensitivity. This is not only because the explosive ablation causes uncertainty in the sample mass removed, but more seriously, the analyte line emissions are always interfered by strong plasma continuum emissions. Signal averaging and time-gated detection are useful solutions. But, for significant improvements, more novel approaches have to be considered.

The strong continuum emissions arise from the high plasma temperature (few electron volts) typically found in laser-induced plasmas.[2−4] As a result, nearly all elements are extensively ionized.[5] The strong analyte lines of neutral atoms are therefore attenuated while the plasma continuum emissions due to the numerous free electrons become overwhelming. The plasma temperature cannot be lowered by simply reducing the laser fluence because a threshold energy density of typically a few Joules per square centimeter is required to induce thermal breakdown.[6] For visible or IR laser ablation at that fluence, the plasma temperature will already reach a few electron volts.[6]

Generally, the ideal plasma temperature to maximize the line-to-background ratio for most atomic analytes is less than one electron volt. In a series of experiments, we have shown that low-temperature (∼0.5 eV) plasmas could be produced by ArF (193-nm) laser ablation of aqueous samples at fluences below the breakdown threshold.[7−9] The continuum emissions were suppressed while the analyte (Na, K, Li, Rb, Ba) line emissions were enhanced. The cooler plasmas were probably produced by photoionization of water molecules when two ArF laser photons were absorbed. This process can be very efficient because vibrationally excited H_2O will absorb resonantly at 193 nm.[10] We have subsequently made use of the extreme sensitivity of 193-nm ablative sampling to measure the amounts of sodium and potassium in single human red blood cells.[11,12]

One is naturally tempted to generalize the technique to sample matrixes other than water, such as solid targets. Since the 1990s, laser ablation has been combined with resonant photoionization to atomize solid samples and selectively ionize the analyte atoms for mass analysis.[13,14] This so-called resonant laser ablation technique proved to be extremely sensitive for solid analysis,[15] although the vacuum requirements and the presumption of analyte identity may compromise its applicability and universality. A possible complementary approach, analogous to our model of ArF laser ablation of aqueous samples, is to tune the wavelength of the ablation laser to resonantly photoionize the abundant host species of the solid matrix instead of the possibly unknown analytes. Electrons will then be freed to impact-excite the guest

* Corresponding author. Fax: 852-2339-5813. E-mail: nhcheung@hkbu.edu.hk

(1) For a recent review of laser-induced breakdown spectroscopy, see Rusak, D. A.; Castle, B. C.; Smith, B. W.; Winefordner, J. D. *Crit. Rev. Anal. Chem.* **1997**, *27*, 257−290.
(2) Majidi, V.; Joseph, M. R. *Crit. Rev. Anal. Chem.* **1992**, *23*, 143−162.
(3) Russo, R. E. *Appl. Spectrosc.* **1995**, *49*, 14A−28A.
(4) Radziemski, L. J.; Cremers, D. A. *Laser-induced plasmas and applications;* Marcel Dekker: New York, 1989.
(5) Houk, R. S. *Anal. Chem.* **1986**, *58*, 97A−104A.
(6) Vertes, A., Gijbels, R., Adams, F., Eds. *Laser Ionization Mass Analysis;* Wiley: New York, 1993; Chapters 3A and 4A.
(7) Cheung, N. H.; Yeung, E. S. *Appl. Spectrosc.* **1993**, *47*, 882−886.
(8) Ho, W. F.; Ng, C. W.; Cheung, N. H. *Appl. Spectrosc.* **1997**, *51*, 87−91.
(9) Ng, C. W.; Ho, W. F.; Cheung, N. H. *Appl. Spectrosc.* **1997**, *51*, 976−983.
(10) Kessler, W. J.; Carleton, K. L.; Marinelli, W. J. *J. Quant. Spectrosc. Radiat. Transfer* **1993**, *50*, 39−46.
(11) Cheung, N. H.; Yeung, E. S. *Anal. Chem.* **1994**, *66*, 929−936.
(12) Ng, C. W.; Cheung, N. H. *Anal. Chem.* **2000**, *72*, 247−250.
(13) McLean, C. J.; Marsh, J. H.; Land, A. P.; Clark, A.; Jennings, R.; Ledingham, K. W. D.; McCombes, P. T.; Marshall, A.; Singhal, R. P.; Towrie, M. *Int. J. Mass Spectrom. Ion Processes* **1990**, *96*, R1−R7.
(14) Borthwick, I. S.; Ledingham, K. W. D.; Singhal, R. P. *Spectrochim. Acta, Part B* **1992**, *47B*, 1259−1265.
(15) Allen, T. M.; Smith, C. H.; Kelly, P. B.; Anderson, J. E.; Eiden, G. C.; Garrett, A. W.; Gill, C. G.; Hemberger, P. H.; Nogar, N. S. *SPIE Proc.* **1995**, *2385*, 39−50.

10.1021/ac991242o CCC: $19.00
Published on Web 03/24/2000

(analyte) atoms at a plasma temperature ideal for emission spectrometry.

However, unlike with aqueous samples, the higher melting and boiling points of solid targets, especially refractory ones, may result in elevated plasma temperatures even near the ablation threshold. Two laser pulses are therefore necessary: the first pulse to ablate and atomize, much like the first spark in the repetitive spark pair of LIBS,[16] and the second pulse to photoionize when the plume has cooled. This is similar to the two-step approach of the so-called laser ablation resonance ionization spectroscopy.[17]

In what follows, by using pellets of potassium iodate as a test matrix, we will show that the extension of resonance-enhanced laser-induced plasma spectroscopy to refractory solid targets is possible, though not straightforward. We will demonstrate that, relative to conventional LIBS, the detection sensitivity could be much enhanced when several critical parameters are optimized. We will also report some preliminary figures of merit.

EXPERIMENTAL SECTION

Crystalline powder of potassium iodate (KIO_3, Ajax) was pressed under 2 000 psi to form cylindrical target pellets. Potassium iodate was chosen for the following reasons: (1) Potassium can be resonantly photoionized by a so-called 1+1 scheme,[18] when a 404.4-nm photon will pump the K atom from the ground $4\ ^2S_{1/2}$ state to the $5\ ^2P_{3/2}$ state while a second 404.4-nm photon will ionize it. The 404.4-nm photon can be conveniently generated by a pulsed dye laser. (2) As a common standard for titrimetric analysis, high-purity KIO_3 is readily available. It is nontoxic, stable, and easy to handle. (3) Upon laser ablation, the iodate is believed to decompose to KI at around 600 °C.[19] The solid iodide is thermally stable and will only vaporize at temperatures above 1300 °C.[20] The pellets are therefore reasonably refractory. (4) The crystalline powder contained a trace amount (17 ppm) of sodium as impurities, which conveniently served as the analyte.

For refractory targets such as the iodate pellets, quite unlike with aqueous samples, extensive thermal ionization became unavoidable even at fluences barely enough to vaporize and atomize the target. This will be shown below. As a result, a double-pulse scheme had to be devised when a relatively intense laser pulse ablated the sample to form a hot vapor plume in air. After a few tens of nanoseconds, when the plume had cooled, a weaker laser pulse at 404.4 nm would intercept the plume to photoionize the abundant K atoms to generate the cool plasma. At the same time, the analyte Na emissions at 589 nm would be monitored.

The experimental setup for the double-pulse scheme is shown schematically in Figure 1.[21] Laser pulses of 5-ns width at a 10-Hz repetition rate from a frequency-doubled Nd:YAG laser (532 nm) were split two ways. One beam was apertured and attenuated with a linear polarizer before it was focused with a 200-mm focal length lens onto the side of a cylindrical pellet of KIO_3. The angle between the ablation beam and the target normal was about 20 degrees. The pellet was rotated continuously in order to present a fresh spot for ablation every time. The other 532-nm beam was mixed with the fundamental (1.06 μm) to generate a 355-nm pulse which was optically delayed before pumping a pulsed dye laser running on Ex-404 (Exciton) dye. The overall delay of the dye-laser output relative to the 532-nm ablation laser pulse was about 30 ns, which was deemed optimal for the vapor plume to cool but not to disperse or react extensively. The dye laser was operated with a spoiled cavity consisting of an external 1200 lines/mm grating assembly in order to broaden the output line width to about 0.2 nm to match the broadened 404.4-nm potassium absorption. The dye-laser output was apertured and attenuated with neutral density filters before it was focused normally with a 200-mm focal length lens onto the same spot on the target.

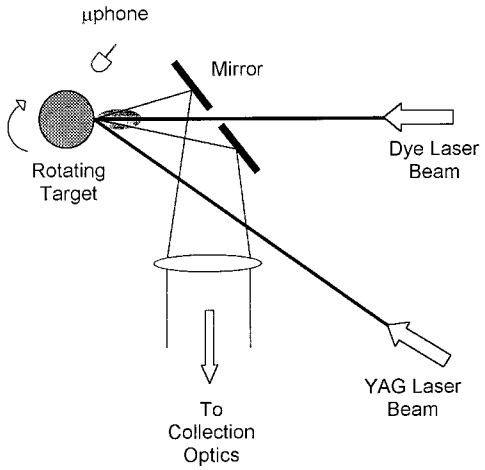

Figure 1. Experimental schematics of the double-pulse scheme are shown. A rotating target of cylindrical pellets of KIO_3 was ablated in air by the second harmonic (532 nm) output of a Nd:YAG laser pulse of 5-ns width; 30 ns later, the expanding plume was intercepted by a dye laser pulse of 5-ns duration and 0.2-nm line width centering on 404.4 nm. The plume emissions were directed onto the entrance slit of a spectrograph equipped with an intensified array detector. The microphone monitored the photoacoustic signal to help track the amount of mass ablated.

Light emissions from the plume were collected axially and directed onto a 200-μm-wide entrance slit of a 0.5-m spectrograph equipped with a 2400 lines/mm grating, giving an overall spectral resolution of about 0.17 nm. An intensified charge-coupled device (ICCD) array detector was mounted at the exit plane of the spectrograph. The intensifier was gateable, and for all the spectra taken, it was gated for 1 μs. The spectral data were stored and processed on a PC. To view the laser-beam profiles at the ablation spot and for ensuring overlap of the two laser beams, the spectrograph grating was turned to zeroth order to act as a mirror, while the ICCD was operated in imaging nonbinning mode. The precision of spatial alignments was better than $\pm$30 μm. Laser beam profiles could be controlled to some extent by focusing as well as by adjusting the aperture size and alignment. At the ablation point, the 532-nm beam spot was found to be fairly circular, with a diameter of about 600 μm at half-maximum intensity. The 404-nm beam spot was more elliptical. The major and minor diameters were, respectively, about 600 μm and 200

(16) Cremers, D. A.; Radziemski, L. J.; Loree, T. R. *Appl. Spectrosc.* **1984**, *38*, 721−729.
(17) Mayo, S.; Lucatorto, T. B.; Luther, G. G. *Anal. Chem.* **1982**, *54*, 553−556.
(18) Hurst, G. S.; Payne, M. G. *Principles and applications of resonance ionisation spectroscopy;* Adam Hilger, Bristol, 1988.
(19) Kroschwitz, J. I., Ed. *Encyclopedia of Chemical Technology*, Volume 19, 4th ed.; Wiley: New York, 1992; p 1084.
(20) NIST Chemistry WebBook, NIST Standard Reference Database, No. 69; National Institute of Standards and Technology: Gaithersburg, MD, Nov. 1998 release.
(21) For further detail on the experimental setup, see Chan, S. Y. Resonance-enhanced laser-induced plasma spectroscopy for elemental analysis. MPhil. Thesis, Hong Kong Baptist University, 1999.

μm at half-maximum intensity. Since we were interested in the minimally invasive regime near the detectability threshold, the typical 532-nm ablation fluence used was low and ranged from 0.5 to 1.3 J/cm^2 (ref 22). The 404-nm laser fluence used ranged from 100 to 700 mJ/cm^2.

To match the dye laser wavelength to the 404.4-nm absorption of potassium, the iodate target was first ablated with 532-nm laser pulses at about 1 J/cm^2. The plume spectrum around 404 nm was captured, and the potassium 404.4-nm and 404.7-nm doublet could be clearly seen. The emission line width was measured to be about 0.3 nm at half-maximum intensity. The target was then irradiated with a much-attenuated dye laser beam, and the scattered light was detected with the ICCD and displayed on the computer screen. The dye laser wavelength was tuned until it overlapped perfectly with the 404.4-nm line of the potassium doublet.

It was useful to track the amount of mass ablated per pulse. For that purpose, a small piezoelectric microphone was placed about 10 mm from the ablation region to monitor the explosion.[23] The microphone output was amplified and displayed on a digital oscilloscope. The etch rate was also measured by weighing the target before and after thousands of ablation pulses.

RESULTS AND DISCUSSION

Single-Pulse Case. Initial attempts were made to ablate the iodate target by using only the dye laser pulse without the 532-nm pre-pulse and to look for enhancement of the sodium 589-nm signal when the dye laser wavelength was tuned from off-resonance (402 nm) to on-resonance (404.4 nm).

As the laser power was increased, the acoustic signal became detectable at a fluence of about 300 mJ/cm^2, which suggested the onset of material ablation. The sodium 589-nm signal was not seen until the laser fluence was increased to about 600 mJ/cm^2, while the dye laser wavelength was set to 404.4 nm. This was shown in Figure 2a (upper trace). The background could be suppressed by gating off the detector during the initial 10 ns. This was shown in the lower trace of the same figure.

With the laser fluence maintained at 600 mJ/cm^2, the dye laser was then tuned off-resonance to 402 nm. The resulting spectra were shown in Figure 2b, where the initial 10 ns was included in the upper trace, but excluded in the lower. As could be seen, the spectra were more or less the same regardless of laser wavelength. With further increase in laser fluence, the spectra remained independent of the wavelength of the dye laser.

The absence of resonance enhancement might be explained if the plasma was largely initiated thermally. Although the theoretical threshold fluence for thermal breakdown was in the Joule per square centimeter range,[6] random hot spots in the laser profile and surface inhomogeneities on the iodate pellets could bring about an early onset of thermal ionization. Strong local fields due to surface inhomogeneities were especially effective in causing desorption and ionization to generate free electrons.[6,24,25] Although

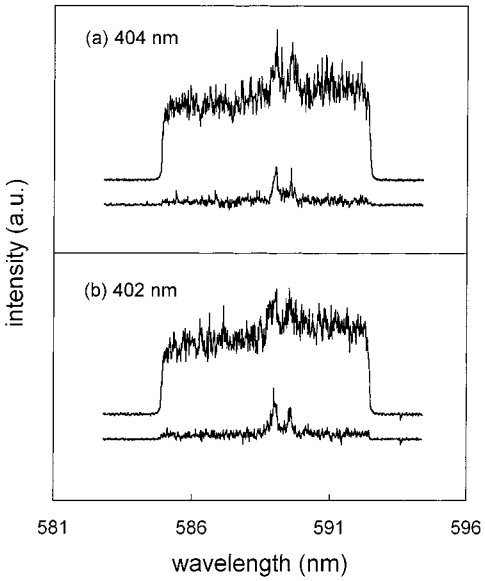

Figure 2. Plume-emission spectra generated by the single-pulse scheme are shown. The KIO_3 pellets were ablated by the dye laser beam alone, at a fluence of about 600 mJ/cm^2. Since the edge pixels of the CCD were not intensified, the spectral trace at the edges served conveniently as a baseline in all cases. (a) The dye laser was tuned to 404.4 nm for resonant K absorption. The emissions were time-integrated for 1 μs, when the initial 10 ns was included (top trace) or excluded (bottom trace) in order to eliminate the continuum background. The two spectral traces were offset vertically for clarity. (b) The dye laser was tuned off-resonance to 402 nm. Spectra with the inclusion (top trace) and exclusion (bottom trace) of the first 10 ns were again shown. As could be seen, the intensity of the sodium doublet did not seem to depend on the wavelength of the dye laser.

local thermal equilibrium might not have been established, an indicative plasma temperature T (eV) could be estimated by using the equation, $T = 3\sqrt{I\lambda\sqrt{\tau}}$, where I is the laser power density (W cm^{-2}), τ is the pulse width (s), and λ is the wavelength (cm).[6] For the case shown in Figure 2, T would be over 1 eV. At that temperature, potassium and sodium atoms would be thermally ionized to a large degree.[5] As a result, thermal ionization dominated over other ionization channels, including photoionization. Whether it was resonant photoionization or not made little difference.

These findings are to be contrasted with those of the case of 193-nm ablation of aqueous samples, when the threshold fluence for vaporization was less than 30 mJ/cm^2, (ref 7) while the threshold fluence for thermal ionization was about 6 J/cm^2(ref 9). The huge fluence window between could be attributed to the low boiling point of water as well as to the uniform and homogeneous surface of liquid targets. The absence of a fluence window for the iodate pellets could well be a problem generally shared among solid targets.

Double-Pulse Case. To overcome the difficulty associated with the lack of proper fluence windows, a hot plasma plume was first created with an intense 532-nm laser pulse. The plume was then allowed to cool before it was intercepted by a nonablative dye laser pulse. Figure 3 shows the double-pulse results. The fluence of the ablative 532-nm pulse was about 1 J/cm^2. The fluence of the dye laser pulse was just below 300 mJ/cm^2, when

(22) All fluences quoted were peak values. For the case of the 532-nm beam, peak fluence was defined as the average fluence of the hottest 100-μm-diameter region at the focal spot. For the case of the dye laser beam, peak fluence was defined as the average fluence of the central 100 μm × 40 μm ellipse. So defined, the peak fluence was about five times the average fluence for both beams. The beam sizes of the central hot region were estimated from the beam overlap data reported in the Results and Discussion.

(23) Lee, K. C.; Chan, C. S.; Cheung, N. H. *J. Appl. Phys.* **1996**, *79*, 3900−3905.
(24) Haglund, R. F., Jr. *Appl. Surf. Sci.* **1995**, *96−98*, 1−13.
(25) Vertes, A.; De Wolf, M. *Anal. Chem.* **1989**, *61*, 1029−1035.

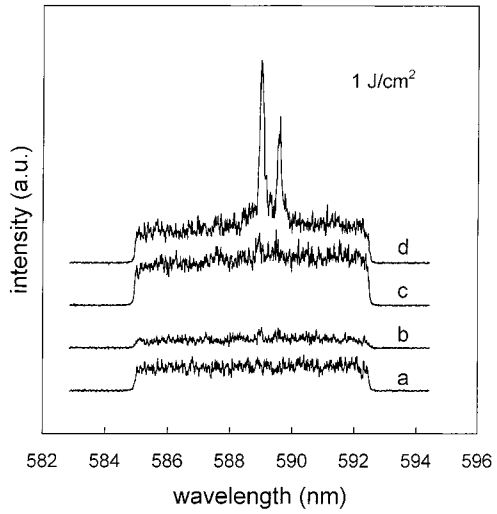

Figure 3. Plume emission spectra generated by the double-pulse scheme are shown. The KIO_3 pellets were ablated by a 532-nm laser pulse at a fluence of about 1 J/cm^2; 30 ns later, the expanding plume was intercepted by a nonablative dye laser pulse of about 300 mJ/cm^2. The plume emissions were time-integrated for 1 μs from the firing of the dye laser. Emission spectra produced by (a) the dye laser alone, (b) the 532-nm laser alone, (c) a 532-nm pulse followed by an off-resonance 402-nm pulse, and (d) a 532-nm pulse followed by an on-resonance 404.4-nm pulse. All four traces were offset vertically for clarity. The resonance enhancement of the Na doublet was clearly seen.

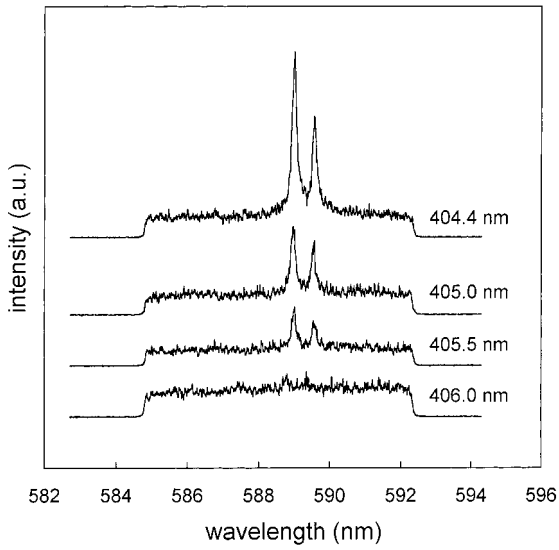

Figure 4. Detuning effect of the dye laser in the double-pulse scheme is shown. Spectral traces were obtained under conditions similar to those of trace (d) in Figure 3, except with progressive detuning of the dye laser away from the resonance wavelength of 404.4 and 404.7 nm. Spectral traces were offset vertically for clarity.

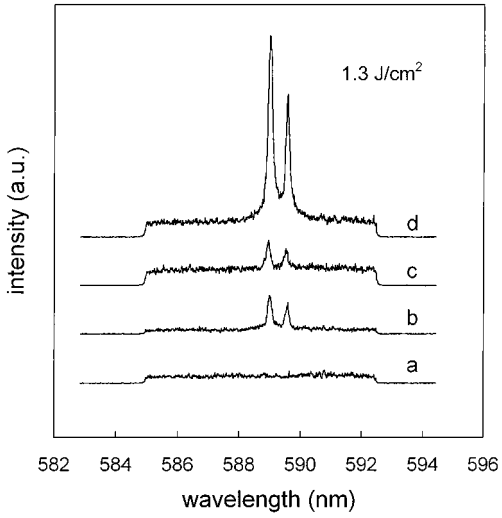

Figure 5. Plume emission spectra generated by the double-pulse scheme. Spectral traces (a) through (d) were obtained under conditions similar to those of the corresponding traces in Figure 3, except with the 532-nm laser fluence increased to 1.3 J/cm^2. When compared with Figure 3, the resonance enhancement could be seen to be equally pronounced.

no acoustic signal was detected, indicating that it was nonablative. The time delay between the two pulses was 30 ns. All spectral traces shown were averages of 300 shots and time-integrated from $t = 0$ (when the dye laser pulse was fired) to $t = 1$ μs, i.e., the first 30 ns since the firing of the 532-nm pulse was excluded to minimize the strong continuum background emissions. Spectral trace (a) in Figure 3 was that obtained with the nonablative 404.4-nm pulse alone. The weak continuum background was attributed to laser-induced fluorescence. Trace (b) was that obtained with the ablative 532-nm pulse alone. Note that the first 30 ns was gated off to eliminate the bright initial flash. The sodium doublet could be seen, though just barely. Trace (c) was with the 532-nm pulse followed 30 ns later by a nonablative and off-resonance 402-nm dye laser pulse. Compared with trace (b), enhancement of the Na emission was not obvious. Trace (d) is similar to trace (c) except that it was obtained with an on-resonance 404.4-nm pulse. The resonance enhancement can clearly be seen.

The resonance behavior of the enhancement is more apparent in Figure 4, in which the detuning effect of the dye laser is shown. It is interesting to note that some enhancement is still discernible with a 1-nm detuning, indicating that the absorption line width may be broader than the 0.3 nm that we had estimated from the 404.4-nm emission line width. Whether the resonance effects can be enhanced still further by broadening the dye laser line width deserves further investigation.

When the fluence of the 532-nm pulse was increased to about 1.3 J/cm^2, the resonance enhancement remained pronounced, as shown in Figure 5, where the spectral traces (a)−(d) bear similar meaning to those shown in Figure 3. Enhancement was also found to increase, approximately linearly, with the fluence of the dye laser in the 100−400 mJ/cm^2 range. Beyond that, the dye laser became too ablative. This linear increase was not consistent with the estimated saturation fluence of 140 mJ/cm^2, (ref 26) presumably because our experimental conditions were far from the ideal assumed in the theoretical estimate.

Interestingly, the enhancement effect was found to depend very critically on the beam profile of the 532-nm laser pulse at the target site. This is shown in Figure 6, when the profiles of the 532-nm beam were made different while the pulse energies were adjusted to give similar background spectral traces to that shown in Figure 3b. The top trace in Figure 6 shows a typical resonance-enhanced Na spectrum. The inset shows the corresponding beam profile that featured a circularly symmetric intensity distribution with a broad "shoulder". When the hot region was shifted off-center, as

(26) Saloman, E. B. *Spectrochim. Acta, Part B* **1993**, *48B*, 1139−1171.

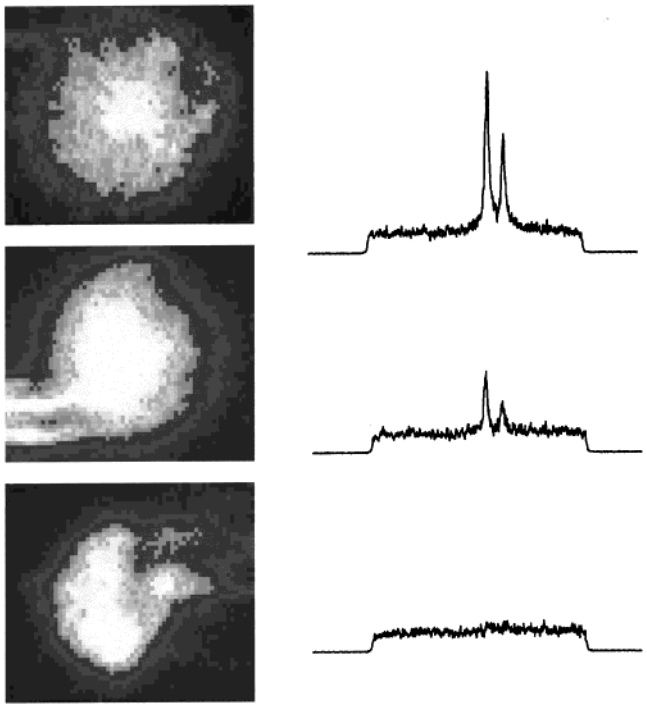

Figure 6. Beam profile effect of the 532-nm laser pulse is illustrated. The emission spectra of the sodium doublet was captured under conditions similar to those of trace (d) in Figure 3, except with three different kinds of 532-nm beam profiles. The CCD images of the beam pattern were shown alongside. Top: A circularly symmetric profile with a broad "shoulder" that gave the largest enhancement. Middle: A more "top-hat" pattern with reduced "shoulder" that gave reduced enhancement. Bottom: A lopsided pattern with the hottest region near the lower edge, when enhancement was no longer apparent.

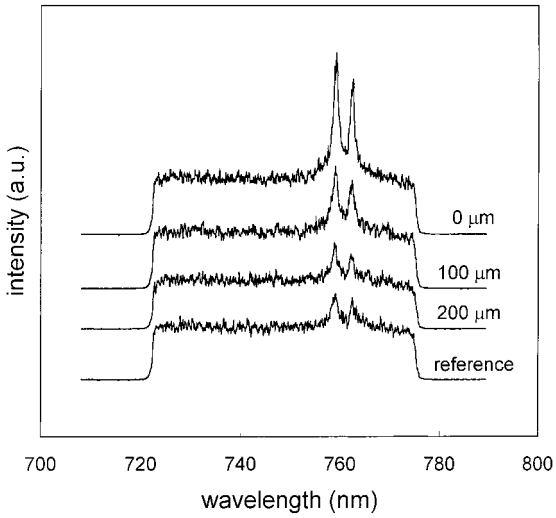

Figure 7. Beam overlap effect is shown. The emission spectra of the potassium 766- and 769-nm doublet were obtained under conditions similar to those of trace (d) in Figure 3, except with various offsets of the 532-nm and 404-nm laser beams, as shown. The bottom trace was the sum of two spectra. One was generated by the 532-nm beam alone. The other was produced by the 404-nm beam alone. Their superposition served as a reference spectrum for enhancement considerations. All traces were offset vertically for clarity.

shown in the bottom inset, the enhancement was completely lost. Even with the circular symmetry left intact but with the shoulder reduced, i.e., a more "top hat" profile (middle inset), enhancement was still reduced, as shown in the corresponding trace in Figure 6.

The dependence of the enhancement on the spatial overlap of the two beams was also far more sensitive than expected. This is illustrated in Figure 7, when the K 766- and 769-nm emissions were monitored while the beam offset was varied. Because of the sensitive dependence on beam overlap, K instead of Na emissions were monitored for better reproducibility. The bottom trace (Figure 7) was the sum of two spectra. One was produced by the 532-nm beam alone. The other was produced by the 404-nm beam alone. Their superposition served as a reference spectrum for enhancement considerations. The top three traces were generated by the double-pulse method, at various beam offsets, as shown. For beam sizes of about 600 μm in diameter at half-maximum intensity, lateral mismatch of the YAG and dye (along the major axis) laser beams by as little as 200 μm would eliminate most of the enhancement effects. Sodium emissions, though less reproducible, were found to decay at about the same rate.

The sensitive dependence on beam profile and spatial overlap might have to do with the small size of the plasma core where resonance enhancement took place, while the relatively thick plume−air interface was dark and nonemitting. This dark protective sheath was somehow needed to buffer the emitting core, possibly by shielding the reactive alkali atoms from the atmosphere or by leveling the otherwise steep gradients of temperature and charge density across the plume−air interface. Elimination of this buffer, either because of poor beam profiles or beam offsets, would suppress the enhancement effect.

Because of the many possible configurations, the analytical performance of this double-pulse technique should be systematically investigated for further optimization. But in order to illustrate, in a preliminary fashion, the sensitivity of the resonance technique, the mass detection limit was estimated as follows. Pellets made from purer potassium iodate powder (Acros, 1.25 ppm Na) were ablated. The fluence of the 404.4-nm beam was held constant at about 300 mJ/cm^2. The fluence of the 532-nm beam, with the profile optimized, was gradually reduced until the sodium doublet was just observable in the resonance-enhanced spectrum, when 200 events were averaged. By "just observable", we mean the ratio of the sodium signal to the background noise (S/N) was estimated to be about three. Sodium signal was defined as the average intensity under the sodium doublet minus the average background intensity. Noise was defined as the standard deviation in the background intensity. The corresponding etch rate was about 800 ng per pulse, as measured with an electronic balance before and after thousands of shots. In other words, at least 1 pg of Na had to be ablated per pulse, and 200 such events had to be accumulated before an S/N of about three could be established. In a similar way, without resonance enhancement, i.e., with the 532-nm pulse alone, 5 pg of Na would need to be ablated per pulse. A five-times enhancement in detection sensitivity was therefore demonstrated.

CONCLUSION

We have generalized the technique of resonance-enhanced laser-induced plasma spectroscopy to refractory targets. By using potassium iodate as a test matrix and the small amount of sodium impurity as test analyte, we have performed laser ablative sampling

using both single-pulse and double-pulse ablation schemes. In the single-pulse scheme, the sample was ablated with a dye laser pulse tuned to 404.4 nm for resonant photoionization of K. But quite unlike the case of 193-nm ablative sampling of aqueous specimens, it was not possible to induce a cool plasma over the iodate target because the fluence window between vaporization and thermal breakdown was too narrow. The difficulty was overcome by using the double-pulse approach. Ablation by an intense 532-nm prepulse produced a hot plasma plume first. After about 30 ns, the cooled plume was intercepted by a second 404.4-nm dye laser pulse. Enhancement of the sodium 589-nm line emissions was then observed. Using the double-pulse scheme, the mass detection limit for Na was about five times lower than that achieved by simply using the 532-nm pulse alone. Because of the many possible combinations of experimental configurations, including beam characteristics and gas ambients, we anticipate still larger enhancement after more systematic optimization.

It should be pointed out that the recent success of 193-nm ablative sampling of aqueous targets is particularly noteworthy when one realizes that water is the common denominator of practically all biological specimens. Common denominators such as silicon, for microelectronics and geological samples, and iron, for the steel industries, are equally important. The technique of double-pulse resonant ablative sampling may prove useful for the elemental analysis of these refractory samples.

ACKNOWLEDGMENT

We thank J. D. Wu for helping with the detection-limit measurements. This work was supported by a Faculty Research Grant from Hong Kong Baptist University.

Received for review November 1, 1999. Accepted February 8, 2000.

AC991242O